Veterinary Pathology
2015, Vol. 52(3) 476-488

DOI: 10.1177/0300985814541705
vet.sagepub.com

Naturally Acquired Bovine Besnoitiosis: Histological and Immunohistochemical Findings in Acute, Subacute, and Chronic Disease

M. C. Langenmayer[1], N. S. Gollnick[2], M. Majzoub-Altweck[1], J. C. Scharr[3], G. Schares[4], and W. Hermanns[1]

Abstract

The pathogenesis of bovine besnoitiosis, a disease of increasing concern within Europe, is still incompletely understood. In this study, disease progression after natural infection with the causative apicomplexan *Besnoitia besnoiti* was monitored in histological skin sections of 5 individual female cattle over time. High-frequency skin sampling of 2 cattle with mild and 2 with severe acute, subacute, and chronic besnoitiosis, as well as from 1 animal during subclinical disease, enabled documentation from the beginning of the disease. Skin sections were stained with hematoxylin and eosin and Giemsa, periodic acid–Schiff reaction, and anti-*Besnoitia* immunohistochemistry. In all 4 clinically affected animals, tachyzoite-like endozoites could be detected for the first time by immunohistochemistry, and tissue cyst evolution was monitored. Besnoitiosis-associated lesions were not detected in the animal showing the subclinical course. Because of the inconsistency of the nomenclature of *Besnoitia* tissue cyst layers in the literature, a new nomenclature for *B. besnoiti* cyst wall layers is proposed: tissue cysts consist of a hypertrophied host cell with enlarged nuclei, an intracytoplasmic parasitophorous vacuole with bradyzoites, a sometimes vacuolated inner cyst wall, and an outer cyst wall in more developed cysts. Inner and outer cyst walls can be readily distinguished by using special stains. In 1 animal, extracystic *B. besnoiti* zoites were immunohistochemically detected during the chronic stage. At necropsy, the 2 severely affected cows displayed large numbers of *B. besnoiti* cysts in a variety of tissues, including the corium of the claws, contributing mainly to the development of chronic laminitis in these 2 cases.

Keywords

Besnoitia besnoiti, bovine besnoitiosis, integument, cattle, immunohistochemistry, laminitis, tissue cyst evolution

Bovine besnoitiosis is caused by *Besnoitia besnoiti*, an apicomplexan parasite.[7] In Europe, the protozoal disease is spreading in the cattle population, causing first autochthonous cases also in countries not previously afflicted such as Germany, Hungary, Italy, and Switzerland.[1,16,20,21,30,34,45,46]

The disease can be divided into an acute, a subacute, and a chronic stage.[3,6] In the acute stage, *B. besnoiti* tachyzoites proliferate within vascular endothelial cells, and clinical signs and histological alterations are mainly associated with vascular lesions.[3] In the subacute and chronic stages, bradyzoite proliferation occurs within mesenchymal host cells, resulting in typical tissue cyst formation in a variety of tissues.[3,4,19,35,36,38,49]

Tachyzoites display different antigens compared with bradyzoites, which can be differentiated via serological tests.[17,47] However, differentiation of tachyzoites from bradyzoites in hematoxylin and eosin (HE)–stained histological sections is difficult, and there are no reliable (immuno)histochemical tools to specifically detect tachyzoites so far. Bradyzoites can be identified by using antibodies against a bradyzoite-specific antigen (BAG) also present in the bradyzoites of other apicomplexan parasites (eg, *Toxoplasma gondii* or *Neospora caninum*).[14]

Unless there is an overwhelming presence of tachyzoites in tissue sections, pathological diagnosis of acute besnoitiosis

[1]Institute of Veterinary Pathology at the Centre for Clinical Veterinary Medicine, Ludwig-Maximilians-Universitaet Muenchen, Munich, Germany
[2]Clinic for Ruminants with Ambulatory and Herd Health Services at the Centre for Clinical Veterinary Medicine, Ludwig-Maximilians-Universitaet Muenchen, Munich, Germany
[3]Rammingen, Germany
[4]Friedrich-Loeffler-Institut, Federal Research Institute for Animal Health, Institute of Epidemiology, Greifswald-Isle of Riems, Germany

Corresponding Author:
M. C. Langenmayer, Institute of Veterinary Pathology at the Centre for Clinical Veterinary Medicine, Ludwig-Maximilians-Universitaet Muenchen, Veterinaerstrasse 13, Munich, D-80539 Germany.
Email: langenmayer@patho.vetmed.uni-muenchen.de

Table 1. Overview of *Besnoitia besnoiti*–Affected Simmental Heifers (SA 4, SA 6, and SA 8) and Limousin Cows (SA 20 and SA 22).

Animal ID	Breed	Age, mo	Pregnancy Status	Study Entry (td)	Acute Stage: Start (td)	Acute Stage: End (td)	Seroconversion (td)	Beginning of Chronic Stage (td)	Course of Disease	Location of Infection
SA 4	S	20	np	1	36	47	45	64	Mild	Trial pasture
SA 6	S	19	np	1	29	41	35	67	Mild	Trial pasture
SA 8	S	13	np	1	—	—	73	—	Subclinical	Trial pasture
SA 20	L	53	p	3	Unknown	7	4	27	Severe	Herd-BbGER1
SA 22	L	49	p	51	Unknown	51	<51	63	Severe	Herd-BbGER1

L, Limousin; np, nonpregnant; p, pregnant, S, Simmental; SA, study animal; td, trial day; —,...; -, not applicable.

is difficult to achieve, as dermal histological lesions are nonspecific and tachyzoites can be rare.[49] In the chronic stage, diagnosis of besnoitiosis in cattle that display clinical signs can be easily achieved by demonstration of typical multilayered tissue cysts in HE-stained skin sections.[10,21]

Current knowledge on the pathology of a *B. besnoiti* infection is based on experimental infections in cattle and rabbits,[3,43] reports of subacute or chronic cases,[10,14,20,45] or a synopsis of cases examined in different stages of the disease.[49] However, to our knowledge, as yet there is only a single study that observed the same animals over the course of all stages of bovine besnoitiosis and included histological examinations of tissues during the different stages of infection.[3] Basson et al[3] used cattle experimentally infected with billions of parasites originating from cell culture or blood or tissue samples to study the evolution of *B. besnoiti* tissue cysts in bovine skin sections and associated pathological findings. According to their definition, the acute stage lasted until termination of dermal edema (3–25 days postinfection), and the chronic stage started with demonstration of mature cysts >300 µm in diameter (>70 days postinfection). The subacute stage was in between and was mainly characterized by cyst evolution. Further studies analyzing naturally infected cattle histologically from the acute to the chronic stage do not exist.

This study was part of a larger study on bovine besnoitiosis disease progression and transmission. We hypothesized that different parasitic stages of *B. besnoiti* and associated lesions can be demonstrated in tissue sections with histological tools even after natural infection, which presumably involves much lower parasite numbers than experimental infection.[3] Therefore, the objective of the study was to investigate naturally acquired bovine besnoitiosis via histology and immunohistochemistry in skin sections of the same animals over a long period with special emphasis on early stages of the disease. Furthermore, we monitored the transition to the subacute and chronic stages of the disease and linked these findings to serological and polymerase chain reaction (PCR) results of already published data on these animals.[48]

Material and Methods

Abbreviations

The following abbreviations will be used throughout the manuscript: *das* = days ante seroconversion, *dps* = days post seroconversion, ICW = inner cyst wall, OCW = outer cyst wall, PV = parasitophorous vacuole, SA = study animal, and td = trial day.

B. besnoiti–*Infected Animals*

The animals included in this study were part of a longitudinal study focusing on the different stages and disease progression of naturally acquired bovine besnoitiosis combining data of clinical examinations, histological investigations, and state-of-the-art diagnostic tests (immunoblot, enzyme-linked immunosorbent assay [ELISA], indirect fluorescent antibody test [IFAT], PCR).[48] In brief, 3 Simmental heifers, study animals (SAs) 4, 6, and 8, acquired bovine besnoitiosis during an 84-day cohabitation trial while housed together with chronically *B. besnoiti*–infected cattle. After the acute and subacute phase of disease, SAs 4 and 6 developed mild chronic bovine besnoitiosis. SA 8 became subclinically infected only. SAs 20 and 22, two Limousin cows belonging to Herd-BbGER1,[48] became infected on summer pasture and entered the study on tds 3 and 51 in the acute stage of disease. Subsequent to the subacute stage, both animals developed a severe course of chronic besnoitiosis (Table 1). After completion of the study, animals remained on the premises for fattening or breeding purposes until submitted to slaughter or necropsy. SA 20 and SA 22 were submitted to necropsy 291 and 188 days after study entry, respectively.

Skin Sample Collection and Tissue Preparation

Skin biopsies were taken under local anesthesia in the femoral region or, less often, laterally at the neck. Samples were fixed in paraformaldehyde (4%) for 24 to 48 hours and subsequently embedded in paraffin and plastic.[24] Sections of 5 µm and 2 µm were routinely stained with HE, according to Giemsa and periodic acid–Schiff (PAS), reaction and examined by light

microscopy. Selected skin sections of SA 6, SA 20, and SA 22 taken during subacute and chronic stages were also stained with Masson's trichrome stain and picrosirius red/Alcian blue.

SA 4, SA 6, and SA 8 were sampled twice a week during the 84-day trial. After entering the acute stage, SA 4 was sampled every other day for 3 weeks. SA 6 was sampled daily for the first week after entering the acute stage and every other day in the following 2 weeks. Thereafter, SA 4 and SA 6 were sampled twice a week again. SA 20 was sampled daily from the day of admission for 3 weeks. Thereafter, SA 20 was sampled once a week for the rest of the 84-day trial. Due to its uncooperative behavior, SA 22 was sampled only on trial days 51, 56, 63, 70, and 80.

Tissues collected during necropsy were fixed, embedded, cut, and stained as described above. Sections of claws were decalcified for 1 week before plastic embedding.

Immunohistochemistry

Immunohistochemistry for detection of *B. besnoiti* zoites was performed on skin sections of SA 4, SA 6, SA 8, SA 20, and SA 22 and on selected parenchymatous organs of SA 20 and SA 22 collected during necropsy. Briefly, sections of paraformaldehyde-fixed, paraffin-embedded tissues were cut at 5 µm. Primary antibody was a rabbit antiserum[2] containing polyclonal antibodies against *B. besnoiti*, used at a dilution of 1:2000. Tissues of experimentally infected γ-interferon knock-out mice[21] comprising tachyzoites and skin of cattle with confirmed bovine besnoitiosis, containing bradyzoites within cysts, served as positive controls. An irrelevant primary antibody (polyclonal rabbit anti–*Escherichia coli*, B0357; Dako, Hamburg, Germany) used on tissue-containing parasites served as a negative control. After deparaffinization and blocking with hydrogen peroxide, a blocking step using diluted normal goat serum for 30 minutes was applied. Primary antibody incubation was performed for 60 minutes at room temperature. Secondary antibody (biotinylated goat anti–rabbit immunoglobulin, BA-1000; Vector, Burlingame, CA) incubation lasted for 45 minutes, followed by incubation with ABC-peroxidase (PK-6100; Vector) and diaminobenzidine-hydrochloride as chromogen (DAB, 4170; Biotrend, Cologne, Germany). Tissues were counterstained with hematoxylin, dehydrated, and protected by a coverslip. To exclude cross-reactions with other apicomplexan species, the anti–*Besnoitia* immunohistochemical staining was tested on mouse tissues containing *T. gondii* tachyzoites, which had been made available from another study on toxoplasmosis,[25] and brain tissue from a cat containing *T. gondii* bradyzoites (in both cases, *T. gondii* zoites had been demonstrated in tissue sections via anti-*Toxoplasma* immunohistochemistry), as well as brain tissue from a cattle containing *N. caninum* tachyzoites[50] (dilution 1:1000) and brain tissue from a dog containing *N. caninum* bradyzoites (in both cases, *N. caninum* zoites had been demonstrated in tissue sections via anti-*Neospora* immunohistochemistry), and muscle tissue obtained from a cattle, necropsied at the Institute of Veterinary Pathology, containing a not further characterized *Sarcocystis* species.

Immunohistochemical staining for cellular markers was performed on skin sections from the skin of SA 4, SA 6, SA 20, and SA 22 obtained during the trial period. Briefly, sections of paraformaldehyde-fixed, paraffin-embedded tissues were cut at 5 µm. Primary antibody was a rabbit anti–CD3 antibody (A045201; Dako) for detection of T lymphocytes, a mouse anti–CD79a antibody (M7051; Dako) for detection of B lymphocytes, and a mouse anti–myeloid/histiocyte-antigen-MAC387 antibody (M0747; Dako) for detection of histiocytes.

After deparaffinization, antigen retrieval was performed by using Proteinase K incubation (MAC387) or a microwave treatment (750 W, 2 × 10 minutes) with a Tris buffer at pH 9.0 (CD3, CD79a). Endogenous peroxidase was blocked with hydrogen peroxide, followed by a blocking step using diluted normal goat serum (CD3, CD79a) or normal rabbit serum (MAC387) for 30 minutes. Primary antibody incubation was performed for 60 minutes at room temperature. In the case of CD3, secondary antibody was a biotinylated goat anti–rabbit immunoglobulin (BA-1000; Vector), and secondary antibody for CD79a was a biotinylated goat anti–mouse immunoglobulin (E0433; Dako). Incubation lasted for 45 minutes, followed by incubation with ABC-peroxidase (PK-6100; Vector) and DAB as chromogen (4170; Biotrend). In the case of MAC387, secondary antibody incubation lasted for 45 minutes with a rabbit anti–mouse immunoglobulin conjugated with peroxidase (P0161; Dako), followed by DAB as chromogen (see above). Tissues were counterstained with hematoxylin, dehydrated, and protected with glass coverslips.

Measurement of Maximum Tissue Cyst Diameter

The maximum tissue cyst diameter (MTCD) was measured in all plastic sections containing cysts of SA 4, SA 6, SA 20, and SA 22. The number of sections measured per study animal and the number of cysts in every measured section are depicted in Fig. 13. Measurements were conducted by using a Videoplan image analysis system (Zeiss-Kontron, Jena, Germany) coupled to a light microscope (Orthoplan; Leitz, Stuttgart, Germany) via a color video camera (CCTV WVCD132E; Matsushita, Kadoma, Japan). Images of HE-stained sections were displayed on a color monitor, and after calibration with an object micrometer (Zeiss, Oberkochen, Germany), the profiles of all tissue cysts in the sections were measured planimetrically by circling their contours with a cursor on the digitizing tablet of the image analysis system.

Serological Data

Data from a previous publication have been used to determine *B. besnoiti* serological status.[48] Four serological tests have been performed as previously described[47,48] by applying published cutoffs.[47,48] In IFAT, a positive cutoff titer of 1:200 was used; in both immunoblots, recognition of at least 4 of 10 bands was regarded positive.[47] In the ELISA, a cut-off of Sample-to-

Positive control ratio SP = 1.756 was applied.[48] A positive seroconversion was assumed when at least 3 of the 4 reference tests were positive.[48]

Definitions

B. besnoiti parasites within skin sections were addressed as zoites. Since there are no specific tools to unambiguously identify tachyzoites selectively, zoites located within vessels and/or intraendothelially were addressed as tachyzoite-like endozoites.[1,9,10,31] Zoites inside hypertrophied host cells with distinguishable cyst wall(s) were addressed as bradyzoites.[1,9,10,13,31,40] As soon as a cyst wall was recognizable in one of the used stains or in PAS reaction surrounding a hypertrophied host cell containing a PV with bradyzoites, the term *tissue cyst* was used. Developed cysts refer to tissue cysts with only a small visible margin of host cell cytoplasm due to a maximally enlarged PV containing bradyzoites.

The acute stage was classified according to clinical criteria. Animals had to show fever (body temperature >39.0°C) or at least 2 of the following clinical signs/diagnoses of acute besnoitiosis: depression, conjunctivitis, subcutaneous edema, lymphadenitis, or lameness.[7,31,43,48] As soon as cysts were clinically observed in the scleral conjunctivae, the term *chronic stage* was used (Table 1). The subacute stage was defined as the stage between the end of the acute and the beginning of the chronic stage.

Results

In skin sections of all animals, there was a very mild basal degree of eosinophilic and lymphoplasmacytic inflammation, mainly located around small vessels and capillaries in the superficial dermis and, if present, subcutis.

Other alterations that did not show correlations with known besnoitiosis-derived lesions were demonstrable in varying degrees in sections of all animals: sporadically occurring focal epidermal edema and pigment incontinence as well as dilated sweat glands, with the latter present in every section.

In tissue sections serving as positive controls for *B. besnoiti*, immunohistochemical staining of the PV membrane and the zoites displayed a brown positive signal, labeling membrane and cytoplasm. Tissues in which an irrelevant primary antibody was used as a negative control displayed no positive signals. The polyclonal antiserum did not cross-react with *T. gondii* and *N. caninum* tachyzoites and bradyzoites. A very faint signal was observed with bradyzoites of *Sarcocystis sp*, which was easily distinguishable from the strong signals *B. besnoiti* zoites revealed.

Acute Stage

During the acute stage, all clinically affected animals showed moderate dermal edema with separation of collagen fibers in the papillary layer. In SA 4, dermal edema was detectable in 9 consecutive biopsies, starting 7 *das;* in SA 6, edema was detectable in 10 consecutive biopsies, starting 2 *das;* and in SA 20, edema was detectable in 7 consecutive biopsies, starting 1 *das*. SA 22 displayed dermal edema only on the day of admission (Fig. 1).

Accompanying the edema, multifocal to coalescing, perivascular infiltrates containing moderate numbers of lymphocytes, plasma cells, and eosinophils as well as a few macrophages were demonstrable in all strata of the dermis in all clinically affected animals (Fig. 4). SA 4 and SA 6 displayed low to moderate numbers of infiltrating inflammatory cells, whereas SA 20 and SA 22 displayed moderate to large numbers of infiltrating cells. Dermal inflammation appeared simultaneously with dermal edema and was detected in 6 consecutive biopsies in SA 4 and in 8 consecutive biopsies in SA 6 and SA 20. SA 22 displayed dermal inflammation only on the day of admission (Fig. 1).

Multifocal to coalescing, mild to moderate, acute dermal hemorrhages were detected in 6 consecutive biopsies in SA 4, starting 3 *das;* on 1 day (1 *das*) in SA 6; for 7 days in SA 20, starting 1 *das;* and on the day of admission and 5 days later in SA 22.

In routine stains, tachyzoite-like endozoites were identified only in HE plastic sections of SA 20 on the day of presentation (1 *das*). Two to 5 sections of tachyzoite-like endozoites were identified per PV, which was located inside endothelial cells in the papillary layer of the dermis (Fig. 2). Longitudinally cut tachyzoite-like endozoites displayed a crescent-like shape with eosinophilic cytoplasm and a round basophilic nucleus.

Using immunohistochemistry, tachyzoite-like endozoites were demonstrated in skin sections of SA 4, SA 6, SA 20, and SA 22. Single or groups of up to 7 parasites were located inside a PV within vascular endothelial cells mainly in the papillary layer, whereas only a few were scattered in the reticular layer. Within endothelial cells, closely spaced crescent-shaped tachyzoite-like endozoites produced a typical banana-stalk pattern (Fig. 3). Some zoites were also located in the neighborhood of small vessels.

Immunohistochemically, tachyzoite-like endozoites were demonstrable in 7 consecutive biopsies in SA 4 and SA 6, starting 8 and 3 *das*, respectively. Tachyzoite-like endozoites were demonstrable immunohistochemically for 6 days in SA 20 and for 1 day in SA 22, starting on the day of admission (Fig. 1). In skin sections of SA 4 and SA 6, only a few dermal tachyzoite-like endozoites were detectable, whereas SA 20 and SA 22 displayed many tachyzoite-like endozoites per skin section.

Subacute and Chronic Stages

Edema and dermal infiltration with inflammatory cells subsided a few days after the last immunohistochemical detection of tachyzoite-like endozoites. Cyst formation was already initialized during the acute stage, while tachyzoite-like endozoites were still detectable (Fig. 1).

Tissue cyst evolution. The first evidence of beginning cyst formation was observed via immunohistochemistry. Hypertrophied host cells possessed 1 or 2 round nuclei and displayed a diffuse tan

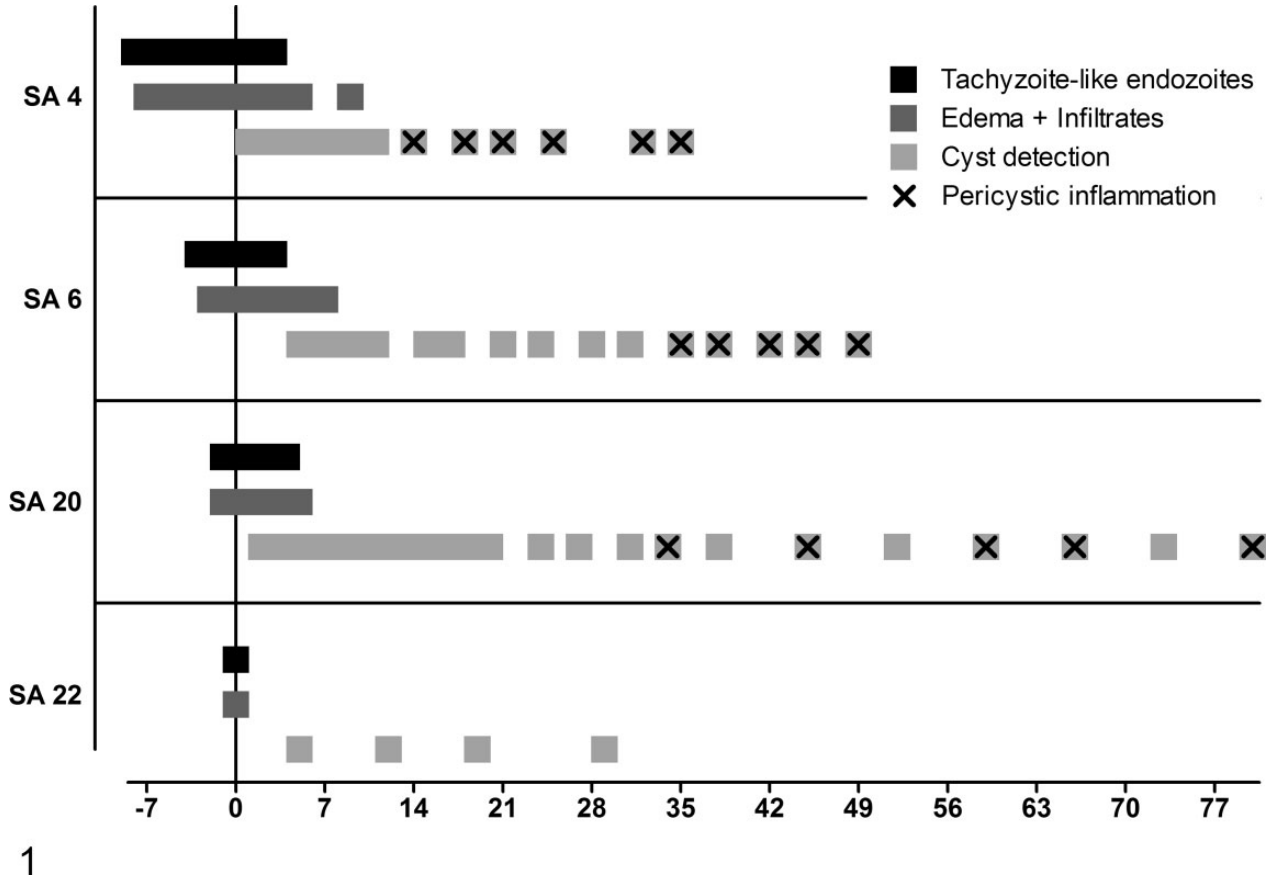

Figure 1. Chronology of histological skin lesions in study animal (SA) 4, SA 6, SA 20, and SA 22. The vertical line depicts day of seroconversion (0) for SA 4, SA 6, and SA 20 and day of admission for SA 22. The x-axis shows the days before (with negative signs) and after seroconversion (S4, SA 6, and SA 20) and day of admission (SA 22).

labeling of the cytoplasm and intense brown labeling of the PV with a single zoite. These hypertrophied host cells had no cyst wall yet, as it was seen later in more evolved tissue cysts.

In HE sections, early tissue cysts consisted of hypertrophied host cells with eosinophilic cytoplasm and 1 enlarged round nucleus containing 1 to 3 nucleoli. The host cells in these young cysts were surrounded by a thin, circular, gray-bluish layer with irregular, lacerated borders, the ICW. The PV was small, taking up about one-fifth of host cell cytoplasm, and contained only a few bradyzoite sections with a crescent- or spindle-shaped eosinophilic cytoplasm and 1 slightly darker nucleus per bradyzoite (Fig. 5).

Tissue cyst evolution commenced by enlargement of the host cell, which contained more hypertrophied round nuclei, each with several nucleoli, and the enlargement of the PV, which contained an increasing number of bradyzoites (Fig. 6). The gray-bluish layer appeared thicker, still expressing an irregular, lacerated outer border, and contained multiple small, clear vacuoles. Especially in plastic sections stained with Giemsa, this layer was colored brightly purple. In sections stained with PAS reaction, the host cell cytoplasm was gray-reddish and sometimes stained brightly PAS positive. The ICW stained violet-reddish, and bradyzoites were gray-violet with several small PAS-positive granules within the cytoplasm of multiple bradyzoites. The ICW stained pale white in Masson's trichrome stain and blue-green in picrosirius red/Alcian blue.

In skin sections of SA 20, taken 20 *dps*, extracystic parasites were detected via immunohistochemistry in 1 location in the papillary and in 1 location in the reticular layer of the dermis. In the papillary layer, several zoites were grouped in a semicircular shape in the periphery of a small vessel; a PV was not detected. In the reticular layer, few zoites were detected intraluminally or associated with the vascular endothelium in a small vessel (Fig. 7). Except for this single biopsy in SA 20, extracystic zoites were not detected after initial intraendothelial proliferation subsided.

Tissue cysts evolved further with consecutive enlargement of the host cells; more host cell nuclei and nucleoli; a larger PV, which still took up only a small part of host cell cytoplasm; and more bradyzoite sections (Figs. 8, 9). Several rounded bodies ranging from 3–4 μm to 11–12 μm, which stained green-grayish in HE-stained sections and brightly positive in PAS reaction, were observed within the PV 38 *dps* in SA 6, 27 *dps*

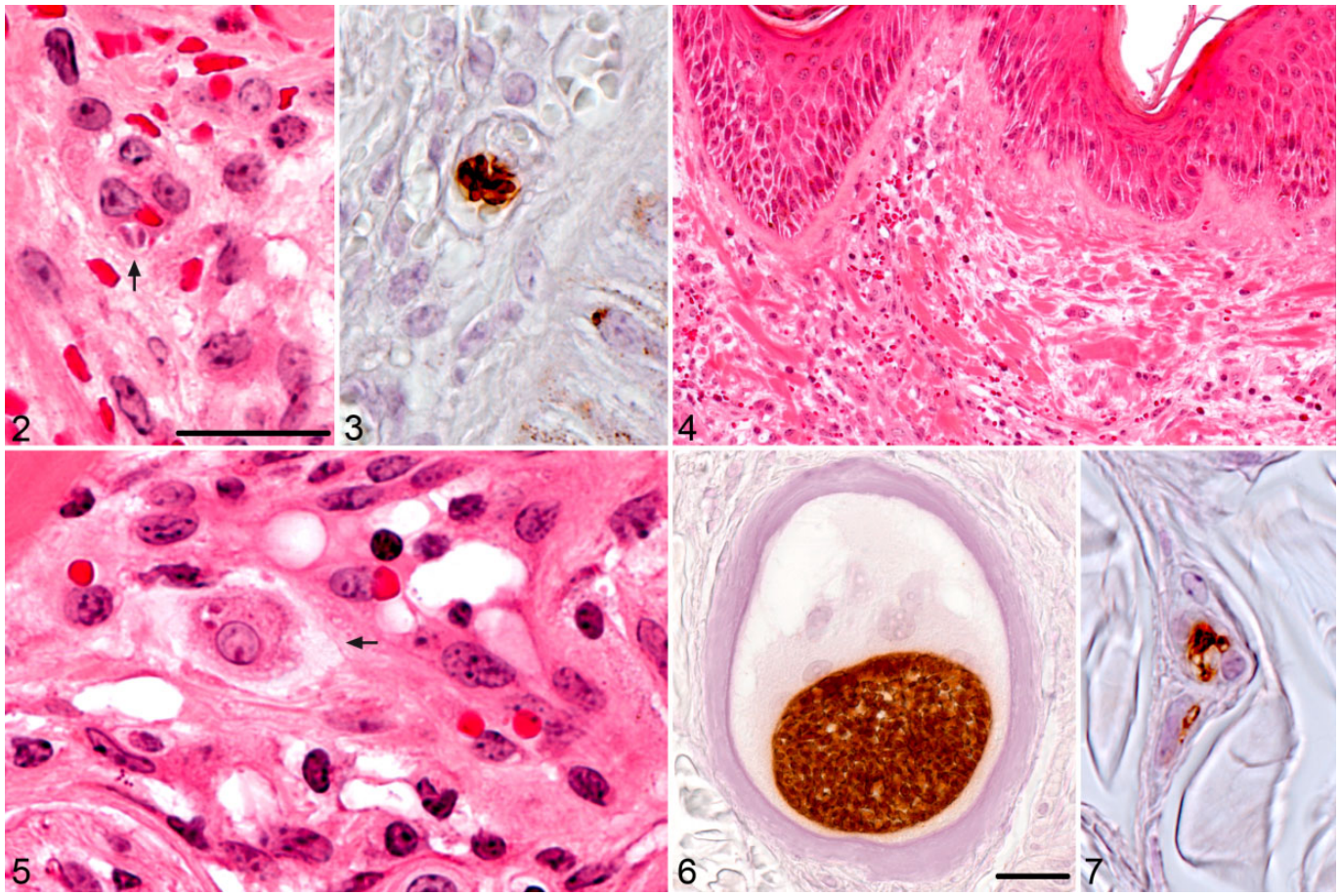

Figures 2–7. *Besnoitia besnoiti* infection, skin, bovine; study animal (SA) 20. **Figure 2.** One day ante seroconversion (*das*). Two *B. besnoiti* tachyzoite-like endozoites inside a parasitophorous vacuole (PV) within a vascular endothelial cell. Bar = 25 μm. Hematoxylin and eosin (HE). **Figure 3.** One *das*. Multiple *B. besnoiti* tachyzoite-like endozoites within a vascular endothelial cell, producing a typical banana-stalk pattern. Same magnification as Fig. 2. Anti-*Besnoitia* immunohistochemistry with hematoxylin counterstain. **Figure 4.** Day of seroconversion. Edema with moderate, perivascular inflammation. HE. **Figure 5.** Four days post seroconversion (*dps*). Very young *B. besnoiti* tissue cyst with hypertrophied host cell and host cell nucleus, PV with 2 bradyzoites, and surrounding inner cyst wall (arrow). Same magnification as Fig. 2. HE. **Figure 6.** Twenty *dps*. *B. besnoiti* tissue cyst with multiple bradyzoites within a PV. Bar = 25 μm. Anti-*Besnoitia* immunohistochemistry with hematoxylin counterstain. **Figure 7.** Twenty *dps*. Few *B. besnoiti* zoites within a small vessel in the reticular layer. Same section as Fig. 6, same magnification as Fig. 2. Anti-*Besnoitia* immunohistochemistry with hematoxylin counterstain.

in SA 20, and 29 days after admission in SA 22. In biopsies taken on the following days and weeks, these bodies were occasionally observed within the PV.

Rarely host cells contained 2 PVs, which were separated by a thin septum of the host cell cytoplasm.

Multiplication of host cell nuclei occurred via endomitosis, producing up to 12 large bizarre mitoses within the host cell cytoplasm. Host cell nuclei showed marked anisokaryosis with a wide array of shapes ranging from simple round or spindle shape to large bizarre nuclei with multiple foldings and invaginations of the nuclear membrane. A maximum of 17 nuclear profiles was counted in a single tissue cyst, containing up to 6 nucleoli per nucleus.

In the periphery of the ICW, a secondary ivory-colored layer, the OCW, began to develop in SA 6, SA 20, and SA 22. Formation of the OCW started with a brightening of the gray-bluish (HE) or violet (Giemsa) ICW or blueing of the pale (Masson's trichrome) ICW from the periphery. In some sections, a patchy pattern of brightening was observed, emphasizing the lacerated borders of the ICW. The OCW was slightly eosinophilic or ivory colored in HE-stained sections; pale white, glassy, and nearly translucent in Giemsa-stained sections; and blue in Masson's trichrome stain. In sections stained with picrosirius red/Alcian blue, the OCW stained red with an orange-colored birefringence in polarized light. A clearly visible OCW was present 35 *dps* in SA 6, 30 days after detection of first cysts; 31 *dps* in SA 20, 29 days after detection of first cysts; and 29 days after admission in SA 22, 24 days after detection of first cysts, before cysts were fully developed. In SA 4, an OCW was not detected.

Cysts were fully developed 49 *dps* in SA 6, 44 days after first cyst detection, and 34 *dps* for SA 20, 32 days after first cyst detection. Developed cysts were not detected in skin sections of SA 4 and SA 22 during the first 84 days of the study. Developed

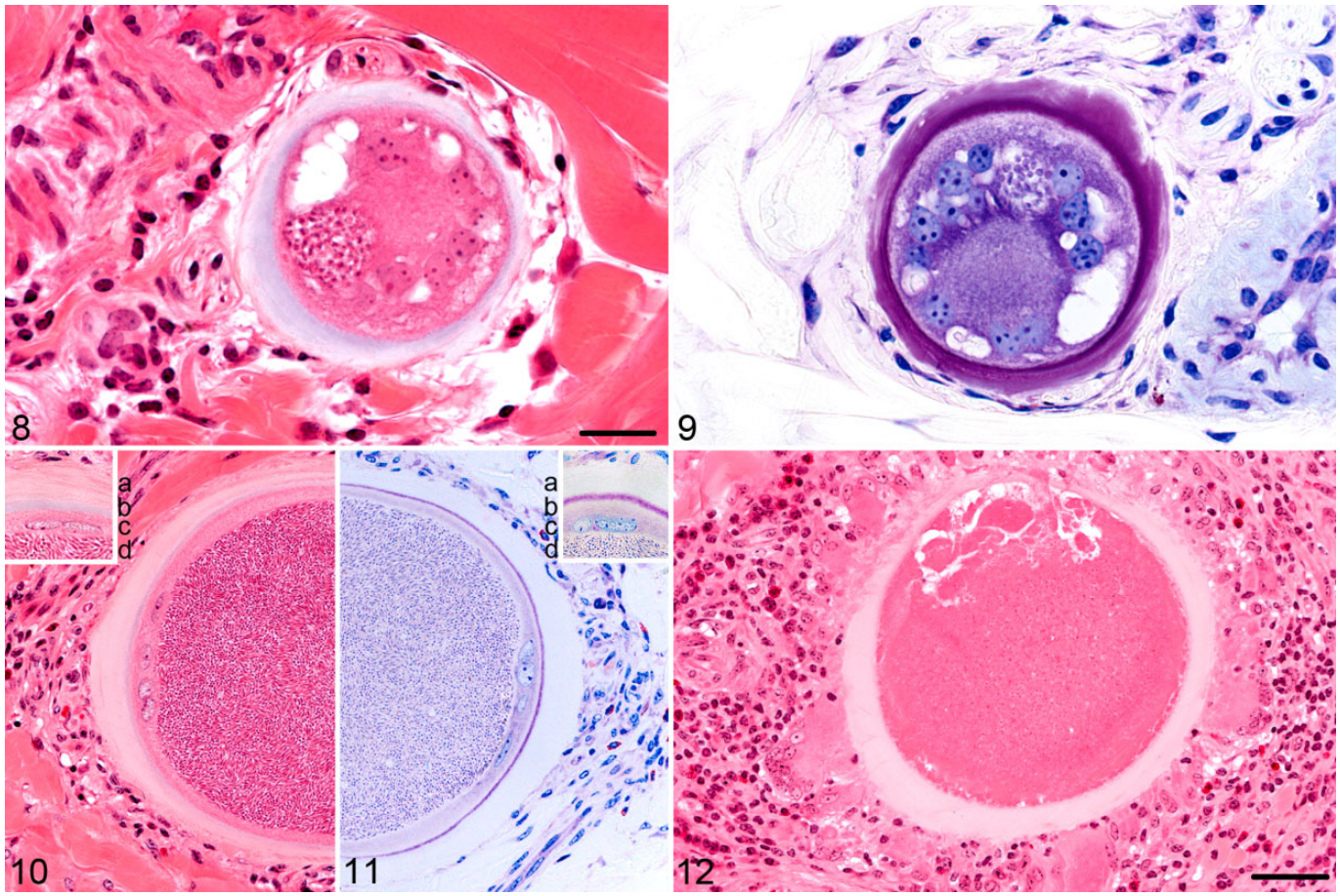

Figures 8–12. *Besnoitia besnoiti* infection, skin, bovine; study animal (SA) 20. **Figure 8.** Twenty-four days post seroconversion (*dps*). *B. besnoiti* tissue cyst with a single parasitophorous vacuole (PV), multiple bradyzoites, host cell nuclei and nucleoli, hypertrophied host cell, and surrounding inner cyst wall (ICW). Bar = 25 μm. Hematoxylin and eosin (HE). **Figure 9.** Twenty-four *dps*. Same cyst as in Fig. 8. Note: Bright purple staining of the ICW. Same magnification as Fig. 8. Giemsa stain. **Figure 10.** Day of necropsy. Developed *B. besnoiti* tissue cyst with maximally enlarged PV, numerous bradyzoites (inset: d), small rim of host cell cytoplasm with flattened host cell nuclei (inset: c), thin rim of the ICW (inset: b), and thick outer cyst wall (OCW; inset: a). Inset: Close-up of the different cyst layers. Same magnification as Fig. 12. HE. **Figure 11.** Day of necropsy. Same cyst as in Fig. 10. Inset: Close-up of the different cyst layers; same captions as in Fig. 10. Note: Thin rim of the purple ICW (inset: b) and pale white, nearly translucent OCW (inset: a). Same magnification as Fig. 12. Giemsa stain. **Figure 12.** Day of necropsy. Lysed *B. besnoiti* cyst with necrotic inner structures and many macrophages, multinucleated giant cells, lymphocytes, and eosinophils in close proximity. Note: Thinning and breaching site of the OCW at the top and cyst-oriented macrophages and multinucleated giant cells directly adjacent to the OCW. Bar = 50 μm. HE.

cysts contained a maximally enlarged, central PV and only a small rim of the host cell cytoplasm surrounding the PV. The host cell nuclei were located in the periphery of the host cell cytoplasm and were flattened. The ICW surrounded the host cell membrane like a thin band. In some sections, the ICW was only merely visible and even sometimes missing. The OCW consisted of several thick eosinophilic laminae surrounding the host cell, with the outermost lamina showing an irregular, lacerated shape blending into the surrounding connective tissue (Figs. 10, 11).

Distribution of tissue cysts. Tissue cysts in the skin were predominantly randomly distributed in the papillary layer, in the direct neighborhood of loose connective tissue. In many sections, tissue cysts were closely arranged together, resulting in coalescing OCWs. Some cysts were detected directly beneath the epidermis, bulging it outward or in the dermal sheath of a hair follicle compressing the outer and inner root sheath of the hair follicle. Intraepithelial cysts were not detected. Only a few cysts were located in the reticular layer and the subcutis, appearing to be lying directly in the periphery of small vessels and loose connective tissue. Some tissue cysts were present in the tunica media of larger vessels, bulging the tunica intima inward into the lumen.

As in the case of tachyzoite-like endozoites, many more tissue cysts were detected in skin sections of SA 20 and SA 22 compared with SA 4 and SA 6, which displayed only a few cysts.

Pericystic inflammation. The immune system of SA 4 and SA 6 already responded to undeveloped tissue cysts. Immune

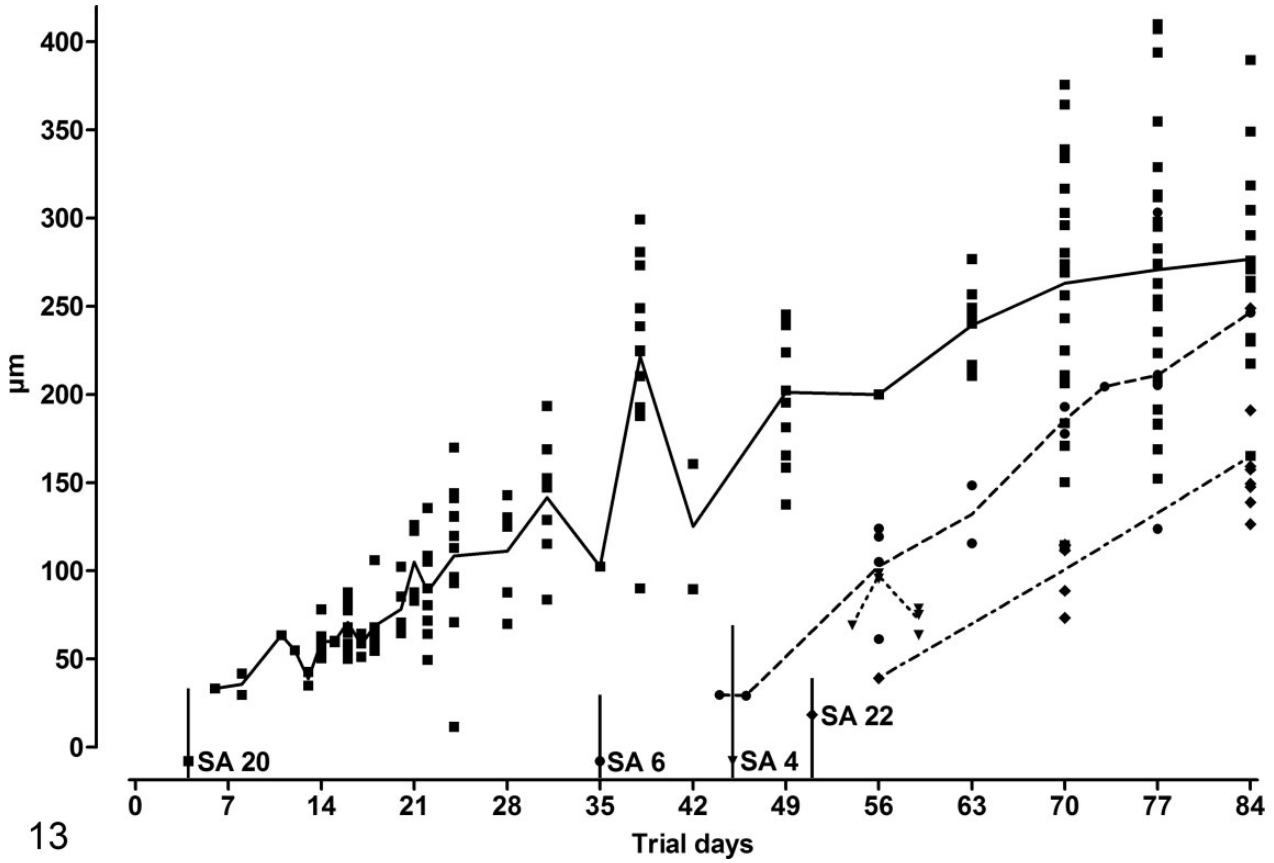

Figure 13. Aligned dot plot of the chronology of mean maximal cyst diameters in plastic skin sections of study animal (SA) 4, SA 6, SA 20, and SA 22. Each replicate represents the diameter of the cyst(s) measured on the respective day. The connecting line represents mean. The vertical lines depict day of seroconversion for SA 4, SA 6, and SA 20 and day of admission for SA 22.

response to cysts in skin sections of SA 20 started after cysts were fully developed. In SA 22, pericystic infiltrates were not found in all 4 biopsies containing tissue cysts. First signs of inflammation surrounding cysts consisted of pericystic infiltration with few lymphocytes, eosinophils, and macrophages. In more pronounced pericystic inflammation, especially the numbers of eosinophils and lymphocytes increased. In severe pericystic inflammation, infiltrates consisted of many lymphocytes, fewer eosinophils and macrophages, and a few multinucleated giant cells of foreign body type (Fig. 12). Macrophages and giant cells adjusted their cytoplasm toward the OCW, displaying a ruffled cytoplasmic border on the cyst side. Tissue cysts without any signs of pericystic infiltrates coexisted adjacent to cysts with mild to marked pericystic inflammation. Immunohistochemistry revealed that pericystic lymphocytes consisted predominantly of T lymphocytes with only a few B lymphocytes scattered in between. The host cell cytoplasm of developed cysts tested negative for CD3, CD79a, and myeloid/histiocyte-antigen (MAC387).

Occasionally, lysis of tissue cysts occurred when pericystic inflammation was breaching the hyaline layer (Fig. 12). Some lysed cysts still contained necrotic debris with only few histiocytic infiltrations; other cysts were completely infiltrated with many histiocytes, eosinophils, and few multinucleated giant cells. In many cases, the OCW was partially intact and displayed a breaching site of variable dimension. Immunohistochemically, intact bradyzoites were not detected in such cysts, but brown granular fragments were observed in the necrotic debris and within the cytoplasm of histiocytes. The first lysis of tissue cysts was observed 25 *dps* in SA 4 and 59 *dps* in SA 6 and SA 20.

In skin sections of SA 8, lesions of acute besnoitiosis (intraendothelial or intravascular tachyzoite-like endozoites, interstitial edema, hemorrhages, or increased perivascular inflammation) were not observed in routine stains and immunohistochemistry in 4 consecutive skin biopsies before and after seroconversion. Lesions associated with chronic besnoitiosis-like tissue cysts or multifocal granulomatous inflammation were not observed in routine stains and immunohistochemistry in skin biopsies taken after seroconversion.

Tissue cyst size. The MTCDs were determined and means calculated for the individual animals and the different time points (Fig. 13). During tissue cyst evolution, mean MTCDs became progressively larger. The smallest MTCD measured out of all animals was 29.3 µm (SA 6, 11 *dps*), and the largest was 409.9 µm (SA 20, 73 *dps*).

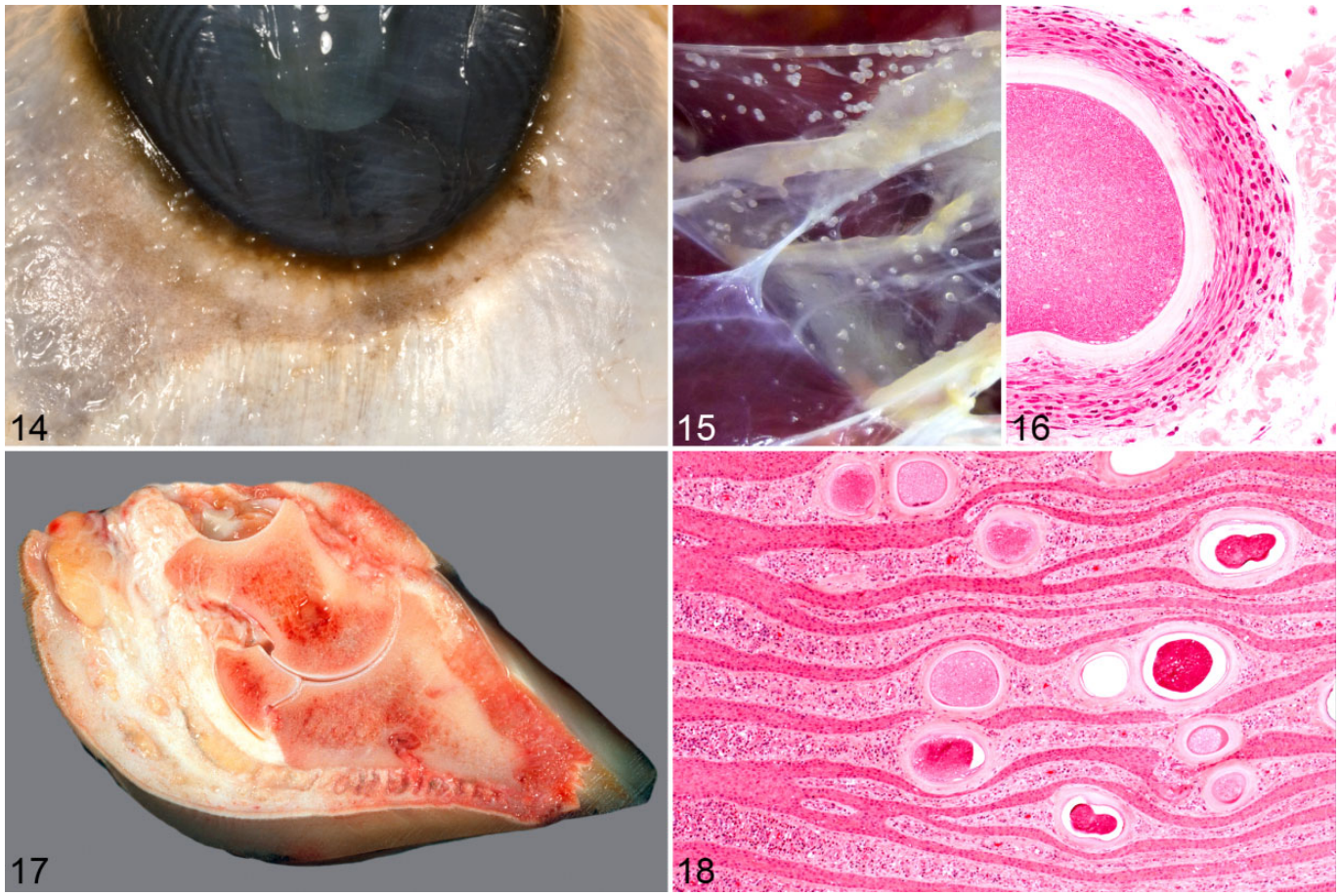

Figures 14–18. *Besnoitia besnoiti* infection; bovine. **Figure 14.** Scleral conjunctiva, study animal (SA) 22 (day of necropsy). Multiple *B. besnoiti* cysts. **Figure 15.** Fascia and muscle, SA 22 (day of necropsy). Multiple *B. besnoiti* cysts in the fascia and muscle of the left hindlimb. **Figure 16.** Fascia, SA 22 (day of necropsy). Histological section of a tissue cyst within fascia with surrounding fibrovascular tissue. Hematoxylin and eosin (HE). **Figure 17.** Claw, SA 20 (day of necropsy). Rotation of the lateral third phalanx of the left forelimb due to chronic laminitis. **Figure 18.** Claw, SA 20 (day of necropsy). Multiple *B. besnoiti* cysts within the lamellae of the laminar corium, causing distention of the lamellae and deviation of the laminar epidermis. Note: Diffuse, subepidermal inflammation. HE.

Necropsy results. At necropsy, the body condition score[15] of SA 20 and SA 22 was 2.5 and 2.25, respectively. The skin was diffusely thickened and seemed less elastic than normal, displaying folds and wrinkles especially in the neck region. The peripheral lymph nodes were enlarged. Multiple, disseminated, miliary white foci, resembling *B. besnoiti* cysts, were observed in the subcutis; musculature; fasciae of the head, neck, trunk, and limbs; mucosa of the entire upper respiratory tract; bronchi; vagina; and scleral conjunctivae (Figs. 14, 15). Single cysts were found in the endocardium of the right atrium and in the splenic capsule in SA 20 and in the veins, especially of the distal limbs, in both animals. Moderate to severe rotation of distal phalanges was present in the claws (Fig. 17). The laminar corium was necrotic in several claws; in single ones, necrotizing inflammation spread to the bone of the distal phalanx, resulting in necrotizing osteomyelitis. In the reticulorumen of SA 22, multiple *Paramphistomum spp* were feeding on the mucosa.

In both animals, developed cysts—many of them with gray-greenish rounded bodies within the PV—with or without pericystic, chronic lymphoplasmacytic, eosinophilic, and granulomatous inflammation were found in a variety of tissues (see below). In tissues exposed to mechanical forces (fascia, skeletal muscle, laminar corium of the claws), the round structure of the tissue cysts displayed impressions, and many cysts showed a more elongated form. Especially in the fasciae, cysts were surrounded by a layer of fibrocytes and vessels directly adjacent to the OCW, which were arranged in a circular fashion around the cysts (Fig. 16).

In the case of SA 20, the lamellae of the laminar corium of the claws were diffusely infiltrated by moderate numbers of lymphocytes, plasma cells, and eosinophils directly beneath the epidermis. In multiple locations, the horn appeared degenerate, and islets of nuclear fragments (possibly neutrophils) were present. In some locations, epidermal infiltration of the inflammatory cells was observed with epidermal edema and keratinocyte necrosis. In both animals, large numbers of *B. besnoiti* cysts were observed in the laminar corium and the sole corium, leading to a distention of the papillae and lamellae of the corium. A deviation or displacement of the infoldings of the

laminar epidermis, especially the lamellae of the *stratum lamellatum*, occurred simultaneously (Fig. 18).

B. besnoiti tissue cysts were observed only within connective tissue and never inside epithelial layers. Extracystic zoites were not detected in parenchymatous organs of either animal via immunohistochemistry.

Sections of the following tissues contained cysts: skin, subcutis, fasciae, muscles, scleral conjunctivae, sclera, nictitating membrane, iris, nasal mucosa, trachea, bronchi, lung, medullary cavity of nasal bones, oral mucosa, salivary glands, vagina, capsule of abdominal hemal lymph node, and small and large vessels. Sections of the following tissues were free of tissue cysts: brain, meninges, thymus, thyroid glands, gastrointestinal tract, liver, pancreas, spleen, kidneys, adrenal glands, uterus, urinary bladder, lens, and cartilage.

Discussion

In this study, cases of spontaneous bovine besnoitiosis in 2 heifers and 2 cows were examined from the acute to chronic stage of infection by histological and immunohistological examinations using paraffin- and plastic-embedded tissues. The high-frequency sampling enabled documentation from the beginning of the disease involving circulating tachyzoite-like endozoites, up to tissue cyst evolution in subacute and chronic stages. To our knowledge, this is the first study conducted on naturally infected cattle over a long period.

There are several important differences between the findings of this study and pathological observations already published.[3,35,49] For the first time, a *Besnoitia*-specific immunohistological approach has been used to detect circulating *B. besnoiti* tachyzoite-like endozoites, which enabled the detection of single tachyzoite-like endozoites during the acute stage, therefore making identification of mild cases possible and enabling detection of extracystic proliferating zoites during the cyst stage as well. Further identification of these zoites as tachyzoites was not conducted, as specific antibodies to selectively identify *B. besnoiti* tachyzoites are lacking, a point that should be addressed in future studies. Furthermore, we described an additional cyst wall layer, resulting in the distinction of 2 cyst wall layers, even in developed cysts. In addition, for the first time, large numbers of tissue cysts were detected in the corium of the claws, which was obviously responsible for the occurrence of a chronic laminitis.

During ongoing chronic besnoitiosis, *B. besnoiti* zoites are usually found only within a PV inside tissue cysts,[3,14] since extracystic proliferation ceases after initial intraendothelial proliferation.[8] Extracystic, intravascular *B. besnoiti* zoites during ongoing chronic besnoitiosis have been described by McCully et al,[36] but they could not fully exclude artificial translocation of bradyzoites into vascular lumina by cutting fresh tissues for histological examination. Schulz[49] reported that bradyzoites, freed from tissue cysts after rupture, can be easily distinguished from artificially translocated ones by the presence of a cellular reaction. Lysis of *B. besnoiti* tissue cysts has been observed in this study as well. However, close to these cysts, no released bradyzoites were observed, and either the content of the cyst was necrotic or the lumen of the cyst was completely filled with cellular infiltrates. In our opinion, it is unlikely that bradyzoites could reach the bloodstream after the lysis of a tissue cyst caused by the cellular immune response because they would have to pass a wall of inflammatory cells. However, intravascular circulation of zoites during the chronic stage may occur after mechanical rupture of tissue cysts lying directly beneath a vascular endothelium or by reactivation of tissue cysts and stage conversion to tachyzoites. Whether the latter occurs in vivo is unknown.[9,14] However, bradyzoites can serve as an infectious agent to produce acute besnoitiosis (and later cyst formation in cattle), as demonstrated in the artificial infection of cattle[7] and laboratory animals.[2,46] Reactivation of chronic rodent besnoitiosis is possible, since it has been demonstrated via experimentally induced immunosuppression in hamsters infected with *Besnoitia jellisoni.*[18]

Both necropsied animals revealed large numbers of tissue cysts in the laminar corium as well as signs of chronic laminitis. The pathogenesis of bovine laminitis is incompletely understood.[22,32,51] However, altered digital blood flow seems to be one of many contributing factors in the development of laminitis.[23,32,51] An attempt to explain equine contralateral limb laminitis evolves around local congestion, slow blood flow, platelet activation, and formation of microthrombi, resulting in inadequate perfusion and ischemia of the lamellar tissue.[32] During the acute stage of bovine besnoitiosis, vascular changes, such as congestion, endothelial injury, edema, and thromboses, are common findings,[3] and reluctance to move and stiff gait are frequently described in diseased animals.[9,31] Combining this information, it is very likely that cattle with acute besnoitiosis display lameness because of acute or subacute laminitis.[23] In chronic besnoitiosis, the presence of tissue cysts within vessel walls of the limbs and within the corium most likely contributes to the development of laminitis. Reduced digital blood flow or localized digital congestion is easy to explain through the presence of multiple tissue cysts in the vessel walls of the distal limbs. Local ischemia may occur because growing and developed tissue cysts compress arteries and capillaries. The multifocal pericystic inflammation may contribute to laminitis as well.[32] Ischemia, compression, and deviation of epithelial lamellae may subsequently lead to production of a horn of minor quality, predisposing the claw to ascending bacterial infection and resulting in sole ulcers or necrotizing laminitis.

Basson et al[3] measured maximum cyst diameter after experimental infection of cattle with *B. besnoiti;* the largest cyst they measured was 390 μm in diameter 77 days postinfection and 66 days after the first appearance of early tissue cysts. In SA 20, the largest cyst (almost 410 μm) was measured 71 days after detection of first cysts. Comparing Basson and others' data with those of the animals in this study, there is a slight deviation by a few days, but the time intervals are similar. The difference in this study between detection of first cysts and first measurement occurred because first cysts were observed in paraffin sections, and measurements have been conducted only in plastic sections to minimize the effect of shrinking artifacts.

A real-time PCR conducted on the skin samples of SA 4, SA 6, SA 20, and SA 22 displayed a decrease in cycle threshold (Ct) values shortly after seroconversion, following a transient increase in Ct values.[48] This suggests a period of increased parasite load within the skin,[48] which coincides with the increase of tissue cyst diameters in this study. Thus, it is very likely that the previously observed decrease in the Ct values reflected the intracystic growth of *B. besnoiti* bradyzoites.

Tissue cysts of *Besnoitia* species differ structurally from cysts of other apicomplexan species. In the literature, nomenclature regarding the composition of *Besnoitia* tissue cysts and cysts walls is not consistent. None of the published schemes[13,26,41,42] were fully applicable when looking at *B. besnoiti* tissue cyst development in this study. Therefore, a new nomenclature that is fully applicable to *B. besnoiti* tissue cysts is suggested: structures within the host cell are called by their respective name—that is, bradyzoites, parasitophorous vacuole, membrane of the parasitophorous vacuole, host cell cytoplasm including organelles and nuclei, and host cell membrane. For the outermost acellular layer, the term *outer cyst wall* is proposed. And for the cyst wall of undeveloped *B. besnoiti* tissue cysts, which, in developed cysts, lies between the OCW and the membrane of the host cell, the term *inner cyst wall* is proposed. The whole hypertrophied host cell, including the ICW and, if present, the OCW, is called a *tissue cyst*.

Interestingly, authors studying developed *B. besnoiti* tissue cysts via light or transmission electron microscopy do not report an ICW or layer between the membrane of the host cell and the OCW.[13,35,37] However, in light microscopic pictures, the ICW can be seen as a blue[37] or slightly eosinophilic layer.[35] Perhaps this layer was interpreted as artifact, occurring after processing of tissues for histological examination. Authors studying *B. besnoiti* tissue cyst development report an ICW directly on the outside of the host cell: a blue layer outside of the host cell, interpreted as a developing cyst wall[3] and a homogeneous capsule enclosing the host cell, staining basophilic in Giemsa-stained sections.[49] Later on they describe that the cyst wall has transitioned into a hyaline[49] or reddish appearance.[3]

The OCW has been studied in several publications with transmission electron microscopy, identifying it as multiple layers of collagen fibrils, arranged in a circular fashion.[13,35,37] Dubey et al[14] studied young *B. besnoiti* tissue cysts in 1 infected bull via electron microscopy, describing the outer layer as a halo with connective tissue elements. The nature of connective tissue elements surrounding the cysts was not reported.

The collagenous nature of the OCW[13,35,37] resulted in a blue staining with Masson's trichrome stain and a red staining with orange-colored birefringence in polarized light in picrosirius red/Alcian blue stain, with the latter suggesting that the OCW is made up of collagen type I fibers.

The ICW, however, did stain pale white with Masson's trichrome stain and blue-green in picrosirius red/Alcian blue, accentuating its different nature. According to the staining reaction of the ICW in the Giemsa and picrosirius red/Alcian blue stain, the ICW is most likely made up of elements of the extracellular matrix (ECM), since other ECM elements (eg, proteoglycans or glycosaminoglycans) show similar staining with the Giemsa or Alcian blue stain as well. This ECM possibly serves as template for the deposition of the collagen fibrils of the OCW. The reason why some developed cysts do not have an ICW may be due to a maximal amount of collagen fibrils deposited within this matrix, connecting the OCW to the host cell membrane. This theory is corroborated by a recent immunohistochemical study on *B. besnoiti* cysts, suggesting myofibroblasts as host cells during cyst stage of *B. besnoiti*,[14] since myofibroblasts are capable of producing both abundant ECM elements and different types of collagen, including collagen type I.[27,33]

The distribution of tissue cysts within the skin and within the whole body is striking. In skin, cysts are more frequently observed in the papillary layer than in the reticular layer. McCully et al[36] suggest this is due to the better vascularization of the papillary layer. They also report that the presence of *B. besnoiti* tissue cysts is associated with small vessels, which is in accordance with the observations in this study, where tissue cysts were noted in the reticular layer of the skin. However, our own observations and that of others show that highly vascularized tissues such as brain, heart, spleen, kidney, or liver do not harbor any or very seldom contain singular cysts.[31,35,36,43] Furthermore, nonintestinal mucosae, fasciae, and subcutaneous and intermuscular loose connective tissue contain large numbers of cysts.[20,35,36] The reason for this distribution pattern is unknown and is often associated with theories of transmission. Shedding of zoites from ruptured cysts in respiratory mucosa to water, grass, or soil[29] and a vertical transmission of parasites found within female genital organs[39] have been suggested. Cysts within the musculoskeletal system make a carnivorous definitive host possible, but several feeding experiments could not determine a definitive carnivorous host.[2,12,44] Superficial dermal cysts favor transmission via direct contact, insects, or inanimate vectors; this mode of transmission has already been shown experimentally.[5,7,43]

Myofibroblasts, recently suggested as host cells in chronic disease,[14] play a key role in physiological tissue repair, ECM deposition, and wound contraction.[11,28,33] In the acute stage of bovine besnoitiosis, dermal inflammation inevitably leads to local cytokine release and changes in ECM elements, which are factors for promotion of myofibroblast differentiation.[27] A promotion of myofibroblasts during acute and subacute stages and subsequent infestation of those cells may be another possible explanation for the distribution pattern of *B. besnoiti* cysts.

The current study is the first to use skin biopsies sampled with high frequency to monitor histological lesions caused by *B. besnoiti* after natural infection. The benefits of this study are the completion of the fragmentary data of morphology of natural bovine besnoitiosis disease evolution, the characterization of tachyzoite-like endozoites using immunohistochemistry during the acute stage, and the detection of extracystic zoites during the ongoing chronic stage, suggesting reactivation of *B. besnoiti* tissue cysts. Furthermore, for the first time, the results depicted here show that lesions of severe chronic besnoitiosis

are correlated with laminitis, which is an important factor for determining the prognosis of severely affected animals.

Acknowledgements

We acknowledge the excellent technical assistance of Teresa Henneke, Elisabeth Kemper, Doris Merl, Michaela Nuetzel, and Heike Sperling. We would like to thank Dr. Walter Basso from Institute of Parasitology, Vetsuisse-Faculty University of Zurich for providing the rabbit antiserum for immunohistochemistry. Further we would like to express our gratitude to the owner of Limousin herd Herd-BbGER1 for his excellent collaboration and support over the years.

Declaration of Conflicting Interests

The author(s) declared no potential conflicts of interest with respect to the research, authorship, and/or publication of this article.

Funding

The author(s) disclosed receipt of the following financial support for the research, authorship and/or publication of this article: The study was financially supported by Prionics AG, Schlieren, Switzerland. NSG was supported by the BGF research stipend provided by the German state of Bavaria.

References

1. Álvarez-García G, Frey CF, Ortega Mora LM, et al. A century of bovine besnoitiosis: an unknown disease re-emerging in Europe. *Trends Parasitol*. 2013;**29**(8):407–415.
2. Basso W, Schares G, Gollnick NS, et al. Exploring the life cycle of *Besnoitia besnoiti:* experimental infection of putative definitive and intermediate host species. *Vet Parasitol*. 2011;**178**(3–4):223–234.
3. Basson PA, McCully RM, Bigalke RD. Observations on the pathogenesis of bovine and antelope strains of *Besnoitia besnoiti* (Marotel, 1912) infection in cattle and rabbits. *Onderstepoort J Vet Res*. 1970;**37**(2):105–126.
4. Besnoit C, Robin V. Les lésions de la sarcosporidiose cutanée des bovins dans leurs rapports avec l'histogénèse du tubercule. *Rev Vét*. 1914;**71**:193–207.
5. Bigalke RD. The artificial transmission of *Besnoitia besnoiti* (Marotel, 1912) from chronically infected to susceptible cattle and rabbits. *Onderstepoort J Vet Res*. 1967;**34**(2):303–316.
6. Bigalke RD. Besnoitiosis and globidiosis. In: Ristic M, McIntyre I, eds. *Diseases of Cattle in Tropics*. The Hague, the Netherlands: Martinus Nijhoff; 1981:429–442.
7. Bigalke RD. New concepts on the epidemiological features of bovine besnoitiosis as determined by laboratory and field investigations. *Onderstepoort J Vet Res*. 1968;**35**(1):3–137.
8. Bigalke RD. The present concept of the life cycle of *Besnoitia besnoiti* of cattle. *J Parasitol*. 1970;**56**(4):29–30.
9. Bigalke RD, Prozesky L. Besnoitiosis. In: Coetzer JAW, Tustin RC, eds. *Infectious Diseases of Livestock*. 2nd ed. Oxford, UK: Oxford University Press; 2004:351–359.
10. Cortes H, Leitao A, Vidal R, et al. Besnoitiosis in bulls in Portugal. *Vet Rec*. 2005;**157**(9):262–264.
11. Desmouliere A, Chaponnier C, Gabbiani G. Tissue repair, contraction, and the myofibroblast. *Wound Repair Regen*. 2005;**13**(1):7–12.
12. Diesing L, Heydorn AO, Matuschka FR, et al. *Besnoitia besnoiti:* studies on the definitive host and experimental infections in cattle. *Parasitol Res*. 1988;**75**(2):114–117.
13. Dubey JP, Shkap V, Pipano E, et al. Ultrastructure of *Besnoitia besnoiti* tissue cysts and bradyzoites. *J Eukaryot Microbiol*. 2003;**50**(4):240–244.
14. Dubey JP, Wilpe E, Blignaut DJC, et al. Development of early tissue cysts and associated pathology of *Besnoitia besnoiti* in a naturally infected bull (*Bos taurus*) from South Africa. *J Parasitol*. 2013;**99**(3):459–466.
15. Edmonson AJ, Lean IJ, Weaver LD, et al. A body condition scoring chart for Holstein dairy cows. *J Dairy Sci*. 1989;**72**(1):68–78.
16. European Food Safety Authority (EFSA). Bovine besnoitiosis: an emerging disease in Europe. *EFSA J*. 2010;**8**(2):1499.
17. Fernández-García A, Álvarez-García G, Risco-Castillo V, et al. Pattern of recognition of *Besnoitia besnoiti* tachyzoite and bradyzoite antigens by naturally infected cattle. *Vet Parasitol*. 2009;**164**(2–4):104–110.
18. Frenkel JK, Wilson HR. Effects of radiation on specific cellular immunities: besnoitiosis and a herpesvirus infection of hamsters. *J Infect Dis*. 1972;**125**(3):216–230.
19. Frey CF, Gutierrez-Exposito D, Ortega-Mora LM, et al. Chronic bovine besnoitiosis: Intra-organ parasite distribution, parasite loads and parasite-associated lesions in subclinical cases. *Vet Parasitol*. 2013;**197**(1–2):95–103.
20. Gentile A, Militerno G, Bassi P, et al. Su di un episodio di besnoitiosi bovina in Italia. *Buiatria J Ital Ass Buiatrics*. 2010;**5**(1):3–15.
21. Gentile A, Militerno G, Schares G, et al. Evidence for bovine besnoitiosis being endemic in Italy: first in vitro isolation of *Besnoitia besnoiti* from cattle born in Italy. *Vet Parasitol*. 2012;**184**(2–4):108–115.
22. Ginn PE, Mansell JEKL, Rakich PM. Skin and appendages. In: Maxie MG, eds. *Jubb, Kennedy, and Palmer's Pathology of Domestic Animals*. 5th ed. 2007.
23. Greenough PR. The laminitis syndrome. In: Bergsten C, Brizzi A, Muelling CKW, eds. *Bovine Laminitis and Lameness*. Philadelphia, PA: Saunders Elsevier; 2007:36–54.
24. Hermanns W, Liebig K, Schulz LC. Postembedding immunohistochemical demonstration of antigen in experimental polyarthritis using plastic embedded whole joints. *Histochemistry*. 1981;**73**(3):439–446.
25. Herrmann DC, Barwald A, Maksimov A, et al. *Toxoplasma gondii* sexual cross in a single naturally infected feline host: generation of highly mouse-virulent and avirulent clones, genotypically different from clonal types I, II and III. *Vet Res*. 2012;**43**(1):39.
26. Heydorn AO, Senaud J, Mehlhorn H, et al. *Besnoitia* sp. from goats in Kenya. *Z Parasitenkd*. 1984;**70**(6):709–713.
27. Hinz B. Formation and function of the myofibroblast during tissue repair. *J Invest Dermatol*. 2007;**127**(3):526–537.
28. Hinz B, Phan SH, Thannickal VJ, et al. The myofibroblast: one function, multiple origins. *Am J Pathol*. 2007;**170**(6):1807–1816.
29. Hofmeyr CFB. Globidiosis in cattle. *J S Afr Vet Med Assoc*. 1945;**16**:102–109.
30. Hornok S, Fedak A, Baska F, et al. Bovine besnoitiosis emerging in Central-Eastern Europe, Hungary. *Parasit Vectors*. 2014;**7**(1):20.

31. Jacquiet P, Lienard E, Franc M. Bovine besnoitiosis: epidemiological and clinical aspects. *Vet Parasitol*. 2010;**174**(1–2):30–36.
32. Katz LM, Bailey SR. A review of recent advances and current hypotheses on the pathogenesis of acute laminitis. *Equine Vet J*. 2012;**44**(6):752–761.
33. Klingberg F, Hinz B, White ES. The myofibroblast matrix: implications for tissue repair and fibrosis. *J Pathol*. 2013;**229**(2): 298–309.
34. Lesser M, Braun U, Deplazes P, et al. First cases of besnoitiosis in cattle in Switzerland [in German]. *Schweiz Arch Tierheilkd*. 2012; **154**(11):469–474.
35. Majzoub M, Breuer W, Gollnick NS, et al. Ein Ausbruch von Besnoitiose bei Rindern in Deutschland: pathomorphologische, ultrastrukturelle und molekularbiologische Untersuchungen. *Wien Tieraerztl Mschr*. 2010;**97**:9–15.
36. McCully RM, Basson PA, Van Niekerk JW, et al. Observations on *Besnoitia* cysts in the cardiovascular system of some wild antelopes and domestic cattle. *Onderstepoort J Vet Res*. 1966;**33**: 245–276.
37. Mehlhorn H, Klimpel S, Schein E, et al. Another African disease in Central Europa: besnoitiosis of cattle. I. Light and electron microscopical study. *Parasitol Res*. 2009;**104**(4):861–868.
38. Nobel TA, Klopfer U, Perl S, et al. Histopathology of genital besnoitiosis of cows in Israel. *Vet Parasitol*. 1981;**8**(4): 271–276.
39. Nobel TA, Neumann M, Klopfer U, et al. Kystes de *Besnoitia besnoiti* dans les organes génitaux de la vache. *Bull Acad Vet de France*. 1977;**50**:569–574.
40. Olias P, Schade B, Mehlhorn H. Molecular pathology, taxonomy and epidemiology of *Besnoitia* species (Protozoa: Sarcocystidae). *Infect Genet Evol*. 2011;**11**(7):1564–1576.
41. Oryan A, Azizi S. Ultrastructure and pathology of *Besnoitia caprae* in the naturally infected goats of Kerman, east of Iran. *Parasitol Res*. 2008;**102**(6):1171–1176.
42. Oryan A, Namazi F, Silver IA. Histopathologic and ultrastructural studies on experimental caprine besnoitiosis. *Vet Pathol*. 2011; **48**(6):1094–1100.
43. Pols JW. Studies on bovine besnoitiosis with special reference to the aetiology. *Onderstepoort J Vet Res*. 1960;**28**:265–356.
44. Rommel M. New knowledge on the biology of Coccidia, *Toxoplasma*, Sarcosporidia and *Besnoitia* [in German]. *Berl Muench Tieraerztl Wochenschr*. 1975;**88**(6):112–117.
45. Rostaher A, Mueller RS, Majzoub M, et al. Bovine besnoitiosis in Germany. *Vet Dermatol*. 2010;**21**(4):329–339.
46. Schares G, Basso W, Majzoub M, et al. First in vitro isolation of *Besnoitia besnoiti* from chronically infected cattle in Germany. *Vet Parasitol*. 2009;**163**(4):315–322.
47. Schares G, Basso W, Majzoub M, et al. Comparative evaluation of immunofluorescent antibody and new immunoblot test for the specific detection of antibodies against *Besnoitia besnoiti* tachyzoites and bradyzoites in bovine sera. *Vet Parasitol*. 2010;**171**(1–2):32–40.
48. Schares G, Langenmayer MC, Scharr JC, et al. Novel tools for the diagnosis and differentiation of acute and chronic bovine besnoitiosis. *Int J Parasitol*. 2013;**43**(2):143–154.
49. Schulz KCA. A report on naturally acquired besnoitiosis with special reference to its pathology. *J S Afr Vet Med Assoc*. 1960;**31**: 21–35.
50. Uzeda RS, Schares G, Ortega-Mora LM, et al. Combination of monoclonal antibodies improves immunohistochemical diagnosis of *Neospora caninum*. *Vet Parasitol*. 2013;**197**(3–4):477–486.
51. Vermunt JJ, Greenough PR. Predisposing factors of laminitis in cattle. *Br Vet J*. 1994;**150**(2):151–164.